distance away from the source of neutron production are going to give erroneous results due to the absorption and scattering of the secondary neutrons. By making use of the experimentally measured neutron fluence and energy distributions from different materials constituting tissue, and combining them in the right proportion, we have estimated the fluence and energies of the secondary neutrons produced by the interaction of C-ions of 100-400 MeV/u energies with patients' tissues. The data is presented in graphical form.

Results:

Our results show that, for a physical treatment dose of 20 Gy in the Brag Peak, the total fluence of secondary nerutrons produced in patients are 1.6 x 10^{9} / cm^{2}, 7.3 x 10^{8} / cm^{2}, 2.5 x 10^{8} / cm^{2} and 4,1 x 10^{7} / cm^{2} respectively at carbon-ions energies of 400,. 300, 200 and 100 MeV / u. The doses to different organs due to these neutrons have also been estimated for the organs in the immediate neighbor -hood of the Bragg Peak, while for far lying organs suggestions are made to compute the respective doses. Our graphical data would help the users of C-ions therapy to select their own "Compromise Optimum energy"

Conclusions:

In our opinion the large number of secondary neutrons produced from patients during therapy with carbon ions, and their corresponding doses to various organs, indicate they could have real potential to cause new primary cancers and cause other harmful side-effects in patients. However, we have provided graphical data which would help to minimise this effect and still make use of any advantage the carbon ions might have in therapy.

QUALITY CONTROL OF YTTRIUM MICROSPHERES FOR MEDICAL APPLICATION

Garibov A.A., Ghahramani M.R., Agayev T.N.
Institute of Radiation Problems, Baku, Azerbaijan

Samples preparation: 200 mgr of each microspheres powder were poured into the quartz ampoules (6Cm height, 0.7 Cm diameter). The quartz ampoules were sealed by oxygen flam. Samples were irradiated inside sealed aluminum containers (7 Cm height, 3 cm diameter) for 10 hours in the research reactor. The medium neutron flux was $3.0 \cdot 10^{13}$ n/ ($sec.cm^{2}$). After cooling time (3 days), the samples were cut and quartz ampoules were crushed, so the activity of samples were measured in the another vials.

Radioactivity: After cooling time, the activity of microspheres measured by curimeter. Figure shows the activity of samples at the different times.

Radiochemical impurity: The radiochemical purity of a radiopharmaceutical is defined as the fraction of the total activity in the desired chemical form in the sample.These impurities arise from incomplete labeling, breakdown of the labeled products over time due to instability, and introduction of extraneous labeled ingredients during synthesis. These impurities cause altered in vivo biodistribution after administration, resulting in an unnecessary radiation dose to the patient. For these reasons, the United States Pharmacopea (USP) and the United States Food and Drug Administration have set limits on the impurities in various radiopharmaceuticals, and these limits must not be exceeded in clinical operations. Radiochemical impurities were checked by two solvent systems: A - saline (NaCl 0.9%) solution as mobile phase (see right-hand plot in Fig. 1),

and B - HCl 0.1 N solution was used as another solvent system (see left-hand plot in Fig. 1). There, chromatography paper sheets are cut into 1Cm*8Cm strips. Around 1 ml of the appropriate solvent is placed into the empty 10 ml glass pharmaceutical vial and two droplet of radioactive solution is spot around 1 cm of the bottom of the strip. After drying droplets, the strips are placed in the appropriate solvent and allow the solvent to migrate until they reach the top of the strip. This procedure generally requires 30 min. After drying the strip, it is cut into 10 pieces (in 1 cm distances) and each segment radioactivity had measured in a beta gamma counter during 1 minute. The beta gamma counter data were expressed in counts per minute (cpm).

The impurities were calculated by expressing the percentage of the activity corresponding to the Rf of the impurity in relation to the total radioactivity on the plate and the radiochemical purity (RCP) was found by subtracting the impurities percentage from 100.

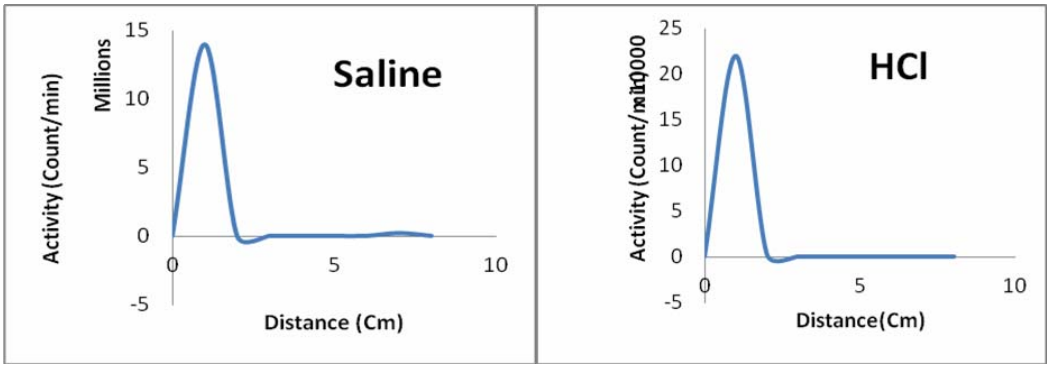

Fig.1. Radiochemical impurities

Tab.1. The gamma-ray spectrum of the irradiated material

Channel	Energy (keV)	FWHM (keV)	Integral	Net Area (Cnts)	Error %	Cps	Suspected Radionuclide
41.74	16.24	1.1463	77265	42663.59	0.86	21.25739	
1230.74	341.75	1.5313	11825	252.81	58.03	0.12596	
1448.55	401.38	1.5915	8218	207.41	60.16	0.10334	
1763.2	487.52	1.675	5106	161.48	60.54	0.08046	La-140
1849.79	511.23	2.8582	9797	2577.75	11.89	1.28438	
3156	868.83	2.003	881	60.4	69.15	0.0301	
3265.42	898.79	2.0267	1108	302.18	16.68	0.15059	
4986.49	1369.97	2.3659	199	67.22	30.86	0.03349	Na-24
5322.63	1461.99	2.4269	167	62.96	29.2	0.03137	
5818.4	1597.72	2.5137	124	67.05	25.68	0.03341	La-140
643597	1766.79	2.6179	18	1.21	723.15	0.0006	
6695.02	1838.72	2.6602	205	162.39	14.28	0.08091	Y-88
7857.15	2155.87	2.8433	5	4.61	181.06	0.0023	

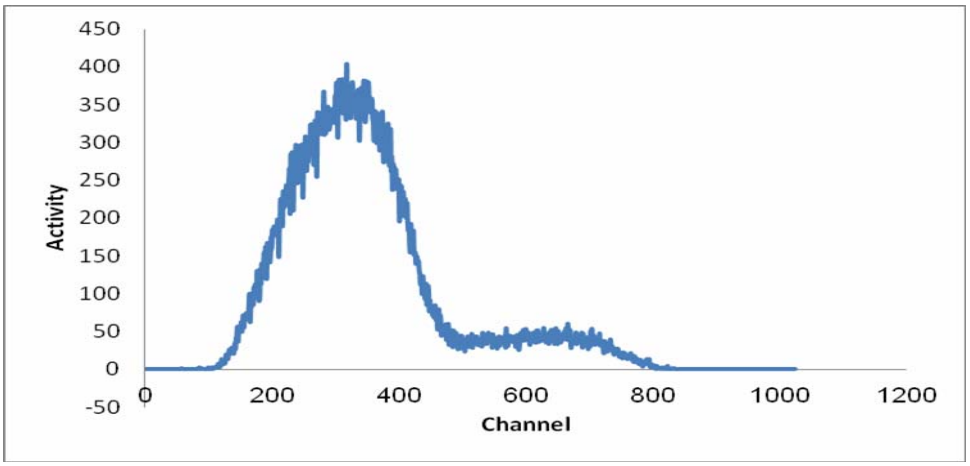

Fig.2. Beta spectroscopy

Radionuclide impurity: The radionuclidic purity of a radiopharmaceutical is the fraction of total activity in the form of the desired radionuclide in the sample. These impurities primarily arise from the radionuclides produced by various nuclear reactions in a target as well as the impurities in the target material. Radionuclide purity of ^{90}Y was checked by two spectrometry system, A: The gamma-ray spectrum of the irradiated material (tab.1). B: Beta spectroscopy depicted a continual spectrum with no unexpected isotopic impurity (Fig.2).

DISCRETE SEMICONDUCTOR COORDINATOR SENSITIVE DETECTOR WITH LARGE-SIZE OF WORKING LAYER

Muminov R.A., Radjapov S.A., Pindyurin Yu.S., Toshmurodov Yo.Q., Risalieva Sh.
Physical-Technical Institute of SPA "Physics-Sun", Tashkent, Uzbekistan

Semiconductor coordinate sensitive detectors (SCSD) on the basis of Si (Li) p-i-n structure it used in recent years as precision devices, especially for experiments in the field of physics of high energy and ecological tasks. Emergence of detectors in the large area was caused by a great interest to them, as coordinate sensitive detectors of large volumes for research of poorly intensive dlinnoprobezhny charged particles and medical a tomograph [1].

This real work is devoted to research discrete coordinate and sensitive detectors of large volumes on the basis of Al-αSi-i-Au.

We have made the structure of detector the indication on fig. 1. For manufacturing p-Si with specific resistance ρ = 5000 Ω·cm, τ =700 μs, from silicon grown up beztigelny zonal melting (BZM) in diameter of 80 mm, and the thickness of d=6 of mm were used. Technology and design of the detector is described in the works [1,2]. On plates were carried out diffusion depth of 500 μm at t=450°C temperature according to the technology [2].

Drift of lithium ions was carried out under temperature T= (80÷90)°C and Voltage of U=(200÷600). With the subsequent low-temperature (T=60°C, U=200B) leveling drift compliance with a mode, offered in the work [3]. After carrying out full compensation of the i-layer, all crystal is exposed to specially chemical and technological processing with a view of